

# Scale invariant survival probability at eigenstate transitions

Miroslav Hopjan<sup>1</sup> and Lev Vidmar<sup>1,2</sup>

<sup>1</sup>*Department of Theoretical Physics, J. Stefan Institute, SI-1000 Ljubljana, Slovenia*

<sup>2</sup>*Department of Physics, Faculty of Mathematics and Physics, University of Ljubljana, SI-1000 Ljubljana, Slovenia*

Understanding quantum phase transitions in highly-excited Hamiltonian eigenstates is currently far from being complete. It is particularly important to establish tools for their characterization in time domain. Here we argue that a scaled survival probability, where time is measured in units of a typical Heisenberg time, exhibits a power-law decay that appears to be independent of system size at eigenstate transitions. We first demonstrate this property in two paradigmatic quadratic models, the one-dimensional Aubry-Andre model and three-dimensional Anderson model. Surprisingly, we then show that similar phenomenology emerges in the interacting avalanche model of ergodicity breaking phase transitions. This establishes an intriguing similarity between localization transition in quadratic systems and ergodicity breaking phase transition in interacting systems.

*Introduction.* Quantum phase transition in highly-excited Hamiltonian eigenstates (shortly, eigenstate transitions) can be seen as a generalization of ground-state quantum phase transitions [1]. They are often characterized by an abrupt change of certain wavefunction properties such as participation ratios or entanglement entropies. Some remarkable consequences of eigenstate transitions may be manifested in nonequilibrium quantum dynamics of isolated quantum systems [2, 3], and may call for refinement of our understanding of quantum chaos [4–6] and thermalization [6–8].

In time domain, the overlap of two time-evolving quantum states may represent a useful probe to study the properties of Hamiltonians that govern the dynamics. Generally, stability of isolated quantum systems against perturbations is studied within the concept of fidelity or Loschmidt echo [9], which became one of the most important tools in the theory of quantum chaos [10, 11] and other areas of physics [11]. Here we focus on survival probability [12], which is the squared overlap of the time evolving state with its initial state. Of particular interest are its properties at intermediate and long times, which may carry nontrivial fingerprints of eigenstate transitions [12–14].

In the context of quadratic Hamiltonians in which eigenstate transitions are driven by disorder, a large amount of previous studies focused on survival probability [12–19]. Perhaps the most important outcomes of these studies are: (i) emergence of a power-law behavior at the eigenstate transition [12–19], and (ii) connecting the power-law exponent to the fractality of the wavefunction [12, 15, 20–25]. It appears that these properties do not crucially depend on whether the quadratic Hamiltonian is local (such as the Anderson and Aubry-Andre models) or it is given by a random-matrix-theory type of models [17, 26]. In spite of these activities, however, it remains unclear whether a quantity such as survival probability may exhibit a scale-invariant behavior at eigenstate transitions that is independent of the details of the underlying quadratic models.

Survival probability in interacting systems has not yet received as much attention as in quadratic systems, apart

from several exceptions [27–31]. However, the quest for exploring the boundaries of thermalization and the emergence of nonergodic phases of matter has recently experienced a tremendous scientific interest [32–34]. It is then an urgent task to establish tools to detect eigenstate transitions through the lens of quantum dynamics, both for single-particle and many-body states.

In the context of interacting systems, it is currently not obvious which are the prototypical models that exhibit an ergodicity breaking phase transition in the thermodynamic limit and are at the same time not subject to severe finite-size effects in numerical analyses. One the most widely studied systems in this respect is the random-field spin-1/2 Heisenberg chain, for which recently different predictions about the fate of ergodicity breaking phase transition have been made [35–62]. A convenient alternative for such studies can be formulated within the so-called avalanche model of ergodicity breaking phase transitions [59, 63–69], which allows for establishing analytical predictions of the value of the transition point [63, 64]. Importantly, numerical results in finite systems comply with these predictions and exhibit only mild finite-size effects [68].

In this Letter, by studying quantum dynamics through the perspective of survival probability, we establish a connection between eigenstate transitions in disordered quadratic systems and ergodicity breaking phase transitions in interacting systems. The central concept of our study is scale invariance of the survival probability, which is observed in both quadratic and interacting systems.

Our analysis consists of two steps. In the first step, we study two paradigmatic quadratic systems, the one-dimensional (1D) Aubry-Andre model and the three-dimensional (3D) Anderson model, and we introduce a scaled survival probability  $p(t)$ , see Eq. (3). This allows us to consider scale invariance of  $p(t)$  as a hallmark of eigenstate transitions. Then we extend our analysis to an interacting system, i.e., to the avalanche model. We show that an identically defined  $p(t)$ , however on many-body wavefunctions, also exhibits scale invariance at the ergodicity breaking phase transition. We relate the power-law exponent of the scale invariant  $p(t)$  to the fractal

dimension of initial states in a chosen basis and the scaling properties of the typical Heisenberg time. Finally, we also discuss a connection of wavefunction based dynamical measures of the transition to the spectrum based measures, such as the spectral form factor.

*Scaled survival probability.* We are interested in quantum quenches from the initial Hamiltonian  $\hat{H}_0$  with eigenstates  $\{|m\rangle\}$  to the final Hamiltonian  $\hat{H}$  with eigenstates  $\{|\nu\rangle\}$ . The eigenstate survival probability for a fixed Hamiltonian realization is defined as

$$P_m^H(t) = |\langle m|e^{-i\hat{H}t}|m\rangle|^2 = \left| \sum_{\nu=1}^D |c_{\nu m}|^2 e^{-iE_\nu t} \right|^2, \quad (1)$$

where we set  $\hbar \equiv 1$ ,  $D$  is the Hilbert-space dimension,  $c_{\nu m} = \langle \nu|m\rangle$  is the overlap of  $|m\rangle$  with  $|\nu\rangle$ , and  $E_\nu$  is an eigenenergy of  $\hat{H}$ . The averaged survival probability is defined as  $P(t) = \langle \langle P_m^H(t) \rangle_m \rangle_H$ , where  $\langle \dots \rangle_m$  denotes the average over *all* eigenstates  $|m\rangle$  of the initial Hamiltonian  $\hat{H}_0$ , and  $\langle \dots \rangle_H$  denotes the average over different realizations of the final Hamiltonian  $\hat{H}$ .

At long times,  $P(t)$  approaches the average inverse participation ratio of eigenstates of  $\hat{H}$  in the eigenbasis of  $\hat{H}_0$ ,  $\bar{P} = \langle \langle \sum_\nu |c_{\nu m}|^4 \rangle_m \rangle_H$ . We express  $\bar{P}$  as

$$\bar{P} = P_\infty + cD^{-\gamma}, \quad (2)$$

i.e., as a sum of the asymptotic value  $P_\infty = \lim_{D \rightarrow \infty} \bar{P}$  and its remainder that vanishes in the thermodynamic limit as  $\propto D^{-\gamma}$ , where  $\gamma$  is the fractal dimension. In the fully delocalized regime one gets  $P_\infty = 0$ , while  $P_\infty > 0$  in the localized regime or the regime with a mobility edge. If the wavefunction at the transition exhibits (multi-)fractal properties, one expects  $\gamma < 1$ .

These considerations allow us to define our central quantity, the scaled survival probability  $p(t)$ , shortly survival probability,

$$p(t) = \frac{P(t) - P_\infty}{\bar{P} - P_\infty}, \quad (3)$$

which saturates at long times to  $\lim_{t \rightarrow \infty} p(t) = 1$ . We study  $p$  in units of scaled time  $\tau = t/t_H^{\text{typ}}$ , where the typical Heisenberg time is  $t_H^{\text{typ}} = 2\pi/\delta E^{\text{typ}}$ , the typical level spacing is  $\delta E^{\text{typ}} = \exp[\langle \langle \ln(E_{\nu+1} - E_\nu) \rangle_\nu \rangle_H]$ , and  $\langle \dots \rangle_\nu$  denotes the average over all pairs of nearest levels.

*Models.* We study two quadratic models with particle-number conservation that exhibit localization-delocalization transitions, given by the Hamiltonian

$$\hat{H} = -t \sum_{\langle ij \rangle} (\hat{c}_i^\dagger \hat{c}_j + \hat{c}_j^\dagger \hat{c}_i) + \sum_{i=1}^D \epsilon_i \hat{n}_i, \quad (4)$$

where  $\hat{c}_j^\dagger$  ( $\hat{c}_j$ ) are the fermionic creation (annihilation) operators at site  $j$ ,  $t$  is the hopping matrix element between nearest neighbour sites,  $\hat{n}_i = \hat{c}_i^\dagger \hat{c}_i$  is the site occupation operator, and  $\epsilon_i$  is the on-site energy. The

first is the Aubry-Andre model on a 1D lattice with  $L$  sites ( $D = L$ ) subject to the quasiperiodic on-site potential  $\epsilon_i = \lambda \cos(2\pi qi + \phi)$ , where  $\lambda$  is the amplitude of the potential,  $q = \frac{\sqrt{5}-1}{2}$  is the golden ratio, and  $\phi$  is a global phase. The model exhibits a sharp localization-delocalization transition at  $\lambda_c/t = 2$  for all single-particle eigenstates [70–80] as consequence of self-duality at the transition. This transition was observed experimentally using cold atoms [81, 82] and photonic lattices [83]. The second is the Anderson model on a 3D cubic lattice ( $D = L^3$ ) subject to the random on-site energies are uncorrelated within box distribution  $\epsilon_i \in [-W/2, W/2]$ . Numerical studies of transport properties of single-particle eigenstates at the centre of energy band [84–86] based on the transfer-matrix technique have shown that the system is insulating for  $W > W_c \approx 16.54t$  [87] and below  $W_c$  it become diffusive [88–90]. At the transition, the model exhibits subdiffusion [88] and multifractal single-particle wavefunctions [91–93]. The transition point is energy dependent, i.e., at  $W > W_c$  all single-particle states are localized, while at  $W < W_c$  the system exhibits a mobility edge [94].

We complement our analysis by studying an interacting model that exhibits an ergodicity breaking phase transition, i.e., the avalanche model [63, 64, 68]. The model consists of  $N + L$  spin-1/2 degrees of freedom in a Fock space of dimension  $D = 2^{N+L}$ . It is divided into a dot with  $N$  spins and a remaining subsystem with  $L$  spins outside the dot, described by the Hamiltonian

$$\hat{H} = \hat{R} + g_0 \sum_{i=1}^L \alpha^{u_i} \hat{S}_{n_i}^x \hat{S}_i^x + \sum_{i=1}^L h_i \hat{S}_i^z. \quad (5)$$

The spins outside the dot are subject to local magnetic fields  $h_i \in [0.5, 1.5]$  that are drawn from a box distribution. Interactions within the dot are all-to-all and they exclusively act on the dot subspace. They are denoted by  $\hat{R}$ , which is represented by a  $2^N \times 2^N$  random matrix drawn from the Gaussian orthogonal ensemble (GOE) [95]. Each of the spins outside the dot is coupled to one spin in the dot. For a chosen spin  $i$  outside the dot, we randomly select an in-dot spin  $n_i$ . The interaction strength is  $g_0 \alpha^{u_i}$ , where  $u_i \in [i - 0.2, i + 0.2]$  is drawn from a box distributions. We set  $N = 3$  and  $g_0 = 1$ , and vary the parameter  $\alpha$ . For these parameters, the transition was found for  $\alpha \approx 0.75$  [68]. For  $\alpha > 0.75$  the model exhibits the GOE energy level statistics [64, 68] and eigenstates are delocalized in Fock space. This can be interpreted as a successful avalanche induced by the dot. For  $\alpha < 0.75$  there is a localization of spins outside a thermal bubble, i.e., a failed thermalization avalanche [69], and the Poisson level statistics emerges [64, 68].

*Initial states.* Unless stated otherwise, the initial Hamiltonian for quadratic models is  $\hat{H}_0 = \sum_i \epsilon_i \hat{n}_i$ , for which the single-particle eigenstates  $\{|m\rangle\}$  in Eq. (1) are fully localized in the site occupation basis. The survival probability can then be interpreted as a quantity that describes the spreading of a particle initially localized in the

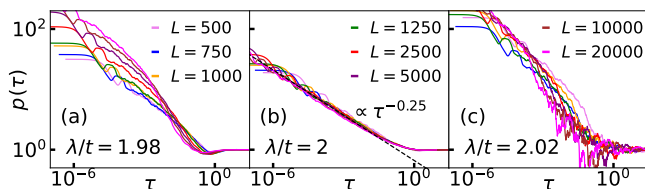


FIG. 1. Survival probability  $p(\tau)$  as a function of the scaled time  $\tau = t/t_H^{\text{typ}}$  in the 1D Aubry-Andree model at different system sizes  $L$ , plotted (a) in the delocalized phase, (b) at the transition point, and (c) in the localized phase. The shaded area in (b) denotes the time-interval of the power-law behavior for the largest system size  $L = 20000$ . The dashed line denotes the fit from Eq. (6) in this regime, yielding  $\beta = 0.25$ .

disordered lattice. For the interacting model the initial Hamiltonian is  $\hat{H}_0 = \hat{R} + \sum_i h_i \hat{S}_i$ . In this case,  $\{|m\rangle\}$  are the many-body eigenstates that describe the ergodic dot uncoupled from the fully localized spins. The survival probability hence tracks the stability of the initially localized spins against the avalanche spreading from the dot.

*Scale invariance at the transition.* We first study the results in quadratic models. In Fig. 1 we show  $p(\tau)$  in the 1D Aubry-Andree model, while Fig. 2 shows  $p(\tau)$  in the 3D Anderson model. At eigenstate transition, see Figs. 1(b) and 2(b), the decay of  $p(\tau)$  appears to be independent of the system size. This scale invariant behavior extends over several orders of magnitude in time, and it is marked by the shaded areas in Figs. 1(b) and 2(b). We fit the functional dependence in this regime by a power-law

$$p(\tau) = a \tau^{-\beta}, \quad (6)$$

where  $a$  and  $\beta$  are fitting parameters. We obtain  $\beta = 0.25$  in Fig. 1(b) and  $\beta = 0.42$  in Fig. 2(b), moreover, in all cases considered in this Letter we obtain  $a < 1$ . Below we discuss the relation of the exponent  $\beta$  to the statistical properties of wavefunctions, specifically the fractal dimension, at the eigenstate transitions. In contrast, when departing from the transition point towards the delocalized regime, see Figs. 1(a) and 2(a), and towards the localized regime, see Figs. 1(c) and 2(c), scaled invariant properties are lost and we do not focus on these regimes further on.

We now ask whether a similar behavior can also be observed in an interacting model, i.e., in the avalanche model. Remarkably, Fig. 3 suggests that this may indeed be the case. Specifically, in Fig. 3(b) we observe scale invariant behavior at the ergodicity breaking transition that is fitted by the power-law from Eq. (6) with  $\beta = 0.31$ . The time interval in which the power-law is observed, see the shaded region in Fig. 3(b), is not as broad as those in quadratic models in Figs. 1 and 2, however, it still extends over nearly two orders of magnitude (see also [96] for details). On the other hand, scale invariance of  $p(\tau)$  is lost in the ergodic phase, see Fig. 3(a), and in the localized phase, see Fig. 3(c).

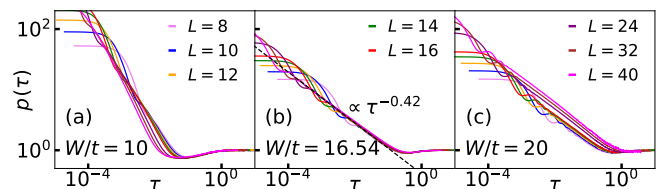


FIG. 2. Survival probability  $p(\tau)$  as a function of the scaled time  $\tau = t/t_H^{\text{typ}}$  in the 3D Anderson model at different system sizes  $L^3$ , plotted (a) in the delocalized phase, (b) at the transition point, and (c) in the localized phase. The shaded area in (b) denotes the time-interval of the power-law behavior for the largest system size  $L = 40$ . The dashed line denotes the fit from Eq. (6) in this regime, yielding  $\beta = 0.42$ .

*Phenomenological description.* We now explore the consequences of the observed scale-invariant behavior at eigenstate transitions. Inserting  $\bar{P} - P_\infty$  from Eq. (2) and the power-law form of  $p(t)$  from Eq. (6) into Eq. (3), and considering its logarithm, one obtains  $\ln(P(t) - P_\infty) = -\beta \ln t + \ln(a(t_H^{\text{typ}})^\beta c D^{-\gamma})$ . We note that if the power-law decay of  $P(t)$  was to extend until  $t = t_H^{\text{typ}}$  [cf. the dashed lines in Figs. 1(b), 2(b) and 3(b)], the value  $P(t_H^{\text{typ}}) - P_\infty$  would be lower than  $cD^{-\gamma}$  since  $a < 1$ . However, our goal is to understand the behavior of  $\beta$ , which corresponds to the slope of the function  $\ln(P(t) - P_\infty)$  versus  $\ln t$ , and hence one can tune the offset of the linear function to set  $P(t_H^{\text{typ}}) - P_\infty = cD^{-\gamma}$ . Scale invariance then allows one to express  $\beta$  by the values of the inverse participation ratio and the typical Heisenberg time at two different system sizes  $L_1$  and  $L_2$ ,

$$\beta = -\frac{\ln[cD(L_2)^{-\gamma}] - \ln[cD(L_1)^{-\gamma}]}{\ln[t_H^{\text{typ}}(L_2)] - \ln[t_H^{\text{typ}}(L_1)]} = \gamma \frac{\ln\left[\frac{D(L_2)}{D(L_1)}\right]}{\ln\left[\frac{t_H^{\text{typ}}(L_2)}{t_H^{\text{typ}}(L_1)}\right]}. \quad (7)$$

The power-law exponent  $\beta$  is hence determined by the fractal dimension  $\gamma$  and the scaling properties of  $t_H^{\text{typ}}$  when expressed in terms of the Hilbert space dimension

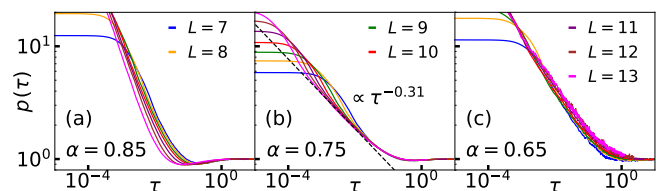


FIG. 3. Survival probability  $p(\tau)$  as a function of the scaled time  $\tau = t/t_H^{\text{typ}}$  in the avalanche model at different system sizes  $L$ , plotted (a) in the delocalized phase, (b) at the transition point, and (c) in the localized phase. The shaded area in (b) denotes the time-interval of the power-law behavior for the largest system size  $L = 13$ . The dashed line denotes the fit from Eq. (6) in this regime, yielding  $\beta = 0.31$ .

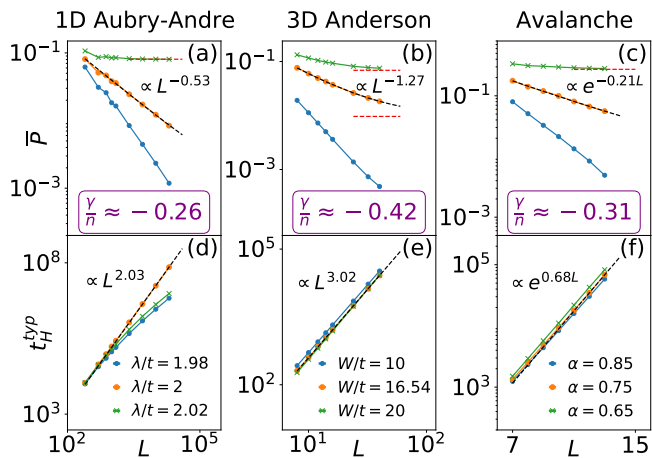


FIG. 4. Scaling of  $\bar{P}$  and  $t_H^{\text{typ}}$  in the models under investigation: (a, d) 1D Aubry-Andre model with  $D = L$ , (b, e) 3D Anderson model with  $D = L^3$ , and (c, f) avalanche model with  $D = e^{(\ln 2)(N+L)}$ . Black dashed lines are fits to the data at eigenstate transitions (circles). (a)-(c): The fractal dimension  $\gamma$  is obtained using Eq. (2), where the horizontal lines denote  $P_\infty$ . At eigenstate transitions we get (a)  $\gamma = 0.532$ , (b)  $\gamma = 0.422$  and (c)  $\gamma = 0.302$ . (d)-(f): The number  $n$  is obtained using Eq. (8). At eigenstate transitions we get (d)  $n = 2.030$ , (e)  $n = 1.007$  and (f)  $n = 0.978$ . The ratios  $\gamma/n$  given in the legends accurately match the values of  $\beta$  from Figs. 1(b), 2(b) and 3(b), in accordance with Eq. (8).

D. We express the latter as

$$\frac{t_H^{\text{typ}}(L_2)}{t_H^{\text{typ}}(L_1)} = \left( \frac{D(L_2)}{D(L_1)} \right)^n \longrightarrow \beta = \frac{\gamma}{n}, \quad (8)$$

where  $n$  is a rational positive number. If the scaling of  $t_H^{\text{typ}}$  with  $L$  is identical to the scaling of the average  $t_H$  with  $L$ , it implies  $n \approx 1$ , but if the spectrum exhibits level clustering or large gaps, they may lead to  $n > 1$ . While Eq. (7) does not distinguish between quadratic and interacting systems, we note that by introducing  $n$  in Eq. (8) for interacting systems, where  $D(L)$  scales exponentially with  $L$ , we neglect multiplicative factors that scale polynomially with  $L$ . Still, as shown below, at sufficiently large  $L$  these contributions can be neglected.

We test predictions from Eq. (8) numerically in Fig. 4. Specifically, we extract  $\gamma$  and  $n$  from the scaling properties of  $\bar{P}$  and  $t_H^{\text{typ}}$  at eigenstate transitions in Figs. 4(a)-4(c) and 4(d)-4(f), respectively, and compare their ratios to the values of  $\beta$  obtained in Figs. 1(b), 2(b) and 3(b), finding excellent agreement. We note that in the 1D Aubry-Andre model, the distribution of level spacings at the transition is anomalous [20]. In Fig. 4(d), we observe  $t_H^{\text{typ}} \approx L^2$ , which justifies the introduction of  $n \neq 1$  in Eq. (8). On the other hand, in the 3D Anderson model, see Fig. 4(b), we observe  $P_\infty \neq 0$  at the transition, which is a consequence of the mobility edge [94] and hence justifies the introduction of  $P_\infty$  to the definition of scaled survival probability in Eq. (3).

*Discussion.* The new results of this Letter can be summarized in two steps. In the first, we established scale invariance of survival probability at eigenstate transitions. The exponent  $\beta$  of the power-law decay in Eq. (6) was linked to the fractal dimension  $\gamma$  and the coefficient  $n$  from the scaling properties of the typical Heisenberg time, see Eq. (8). This allows us to consider scale invariance in two paradigmatic quadratic models, the 1D Aubry-Andre model and the 3D Anderson model, within the same framework. In the second, most important step, we observe that this phenomenology also applies to ergodicity breaking transitions in interacting systems. In this case, the exponent  $\beta$  of the power-law decay is proportional to the fractal dimension  $\gamma$  of the inverse participation ratio of the many-body wavefunction.

The values of fractal dimensions  $\gamma$ , as well as the power-law decay of survival probability, can be seen as being a consequence of a particular choice of the initial Hamiltonian  $\hat{H}_0$ , in which eigenstates are product states in real space. However, since we are studying the transition to localization, such  $\hat{H}_0$  is a natural candidate to allow for a detection of the transition point. For quantum quenches in which initial states are eigenstates of other Hamiltonians, power-law decay may not be guaranteed and hence the question of scale invariance remains open.

Still, in the case of the 1D Aubry-Andre model, the eigenstate transition occurs between states that are localized in quasimomentum space and states that are localized in real space [70, 71]. This suggests that it may also be reasonable to consider plane waves as initial states, since they are completely localized in quasimomentum space. Testing this idea in [96], we again observe a power-law behavior described by Eq. (6), and we obtain  $\beta = 0.27$ . This is only slightly larger than  $\beta = 0.25$  observed in Fig. 1(b) and the corresponding value  $\gamma/n = 0.26$  in Fig. 4(a), eventually suggesting agreement within a numerical precision.

Another interesting open question concerns the relation of survival probability at eigenstate transitions with the statistical properties of Hamiltonian spectra. Recent studies of the spectral form factor (SFF) at eigenstate transitions of the 3D Anderson model [97] and the avalanche model [68] observed a scale-invariant plateau in time domain that extends over several orders of magnitude. Even though survival probability is formally not equivalent to the SFF, certain analogies can be established [98] (see also [96]). It is then reasonable to conjecture in these cases that the scale-invariant plateau in the SFF is related to the scale-invariant power-law decay of the survival probability. In [96] we numerically confirm that both scale-invariant phenomena occur in approximately the same time windows. However, the SFF in the 1D Aubry-Andre model, in contrast to the other two models, exhibits a scale-invariant *power-law* decay at the transition [96]. The latter emerges in nearly the same time window as a power-law decay of the survival probability.

*Acknowledgment.* We acknowledge discussions with P.

Prelovšek and T. Prosen and J. Šuntajs. We acknowledge the support of the Slovenian Research Agency (ARRS), Research Core Fundings Grants P1-0044 and J1-1696. We gratefully acknowledge the High Performance Computing Research Infrastructure Eastern Region (HCP

RIVR) consortium ([www.hpc-rivr.si](http://www.hpc-rivr.si)) and European High Performance Computing Joint Undertaking (EuroHPC JU) ([eurohpc-ju.europa.eu](http://eurohpc-ju.europa.eu)) for funding this research by providing computing resources of the HPC system Vega at the Institute of Information sciences ([www.izum.si](http://www.izum.si)).

- 
- [1] S. Sachdev, *Quantum Phase Transitions* (Cambridge University Press, New York, 2011).
- [2] A. Polkovnikov, K. Sengupta, A. Silva, and M. Vengalattore, Nonequilibrium dynamics of closed interacting quantum systems, *Rev. Mod. Phys.* **83**, 863 (2011).
- [3] J. Eisert, M. Friesdorf, and C. Gogolin, Quantum many-body systems out of equilibrium, *Nat. Phys.* **11**, 124 (2015).
- [4] F. Haake, S. Gnutamann, and M. Kus, *Quantum signatures of chaos* (Springer, 2018).
- [5] H.-J. Stöckmann, *Quantum chaos: an introduction* (Cambridge University Press, 2000).
- [6] L. D'Alessio, Y. Kafri, A. Polkovnikov, and M. Rigol, From quantum chaos and eigenstate thermalization to statistical mechanics and thermodynamics, *Adv. Phys.* **65**, 239 (2016).
- [7] T. Mori, T. N. Ikeda, E. Kaminishi, and M. Ueda, Thermalization and prethermalization in isolated quantum systems: a theoretical overview, *J. Phys. B* **51**, 112001 (2018).
- [8] J. M. Deutsch, Eigenstate thermalization hypothesis, *Rep. Prog. Phys.* **81**, 082001 (2018).
- [9] A. Peres, Stability of quantum motion in chaotic and regular systems, *Phys. Rev. A* **30**, 1610 (1984).
- [10] T. Gorin, T. Prosen, T. H. Seligman, and M. Žnidarič, Dynamics of loschmidt echoes and fidelity decay, *Physics Reports* **435**, 33 (2006).
- [11] A. Goussev, R. A. Jalabert, H. M. Pastawski, and D. A. Wisniacki, Loschmidt echo, *Scholarpedia* **7**, 11687 (2012). Revision #127578.
- [12] R. Ketzmerick, G. Petschel, and T. Geisel, Slow decay of temporal correlations in quantum systems with cantor spectra, *Phys. Rev. Lett.* **69**, 695 (1992).
- [13] S. A. Schofield, P. G. Wolynes, and R. E. Wyatt, Computational study of many-dimensional quantum energy flow: From action diffusion to localization, *Phys. Rev. Lett.* **74**, 3720 (1995).
- [14] S. A. Schofield, R. E. Wyatt, and P. G. Wolynes, Computational study of many-dimensional quantum vibrational energy redistribution. I. Statistics of the survival probability, *J. Chem. Phys.* **105**, 940 (1996).
- [15] R. Ketzmerick, K. Kruse, S. Kraut, and T. Geisel, What determines the spreading of a wave packet?, *Phys. Rev. Lett.* **79**, 1959 (1997).
- [16] M. Gruebele, Intramolecular vibrational dephasing obeys a power law at intermediate times, *Proc. Natl. Acad. Sci.* **95**, 5965 (1998).
- [17] G. S. Ng, J. Bodyfelt, and T. Kottos, Critical fidelity at the metal-insulator transition, *Phys. Rev. Lett.* **97**, 256404 (2006).
- [18] D. M. Leitner, Quantum ergodicity and energy flow in molecules, *Adv. Phys.* **64**, 445 (2015).
- [19] S. Karmakar and S. Keshavamurthy, Intramolecular vibrational energy redistribution and the quantum ergodicity transition: a phase space perspective, *Phys. Chem. Chem. Phys.* **22**, 11139 (2020).
- [20] T. Geisel, R. Ketzmerick, and G. Petschel, New class of level statistics in quantum systems with unbounded diffusion, *Phys. Rev. Lett.* **66**, 1651 (1991).
- [21] B. Huckestein and L. Schweitzer, Relation between the correlation dimensions of multifractal wave functions and spectral measures in integer quantum hall systems, *Phys. Rev. Lett.* **72**, 713 (1994).
- [22] R. del Rio, S. Jitomirskaya, Y. Last, and B. Simon, What is localization?, *Phys. Rev. Lett.* **75**, 117 (1995).
- [23] V. E. Kravtsov, A. Ossipov, O. M. Yevtushenko, and E. Cuevas, Dynamical scaling for critical states: Validity of chalker's ansatz for strong fractality, *Phys. Rev. B* **82**, 161102 (2010).
- [24] V. E. Kravtsov, A. Ossipov, and O. M. Yevtushenko, Return probability and scaling exponents in the critical random matrix ensemble, *Journal of Physics A: Mathematical and Theoretical* **44**, 305003 (2011).
- [25] V. E. Kravtsov, O. M. Yevtushenko, P. Snajberk, and E. Cuevas, Lévy flights and multifractality in quantum critical diffusion and in classical random walks on fractals, *Phys. Rev. E* **86**, 021136 (2012).
- [26] S. Bera, G. De Tomasi, I. M. Khaymovich, and A. Scardicchio, Return probability for the anderson model on the random regular graph, *Phys. Rev. B* **98**, 134205 (2018).
- [27] E. J. Torres-Herrera and L. F. Santos, Dynamics at the many-body localization transition, *Phys. Rev. B* **92**, 014208 (2015).
- [28] E. J. Torres-Herrera, A. M. García-García, and L. F. Santos, Generic dynamical features of quenched interacting quantum systems: Survival probability, density imbalance, and out-of-time-ordered correlator, *Phys. Rev. B* **97**, 060303 (2018).
- [29] P. Prelovšek, O. S. Barišić, and M. Mierzejewski, Reduced-basis approach to many-body localization, *Phys. Rev. B* **97**, 035104 (2018).
- [30] M. Schiulaz, E. J. Torres-Herrera, and L. F. Santos, Thouless and relaxation time scales in many-body quantum systems, *Phys. Rev. B* **99**, 174313 (2019).
- [31] T. L. M. Lezama, E. J. Torres-Herrera, F. Pérez-Bernal, Y. Bar Lev, and L. F. Santos, Equilibration time in many-body quantum systems, *Phys. Rev. B* **104**, 085117 (2021).
- [32] R. Nandkishore and D. A. Huse, Many-body-localization and thermalization in quantum statistical mechanics, *Ann. Rev. Cond. Mat. Phys.* **6**, 15 (2015).
- [33] E. Altman and R. Vosk, Universal Dynamics and Renormalization in Many-Body-Localized Systems, *Ann. Rev. Cond. Mat. Phys.* **6**, 383 (2015).
- [34] D. A. Abanin, E. Altman, I. Bloch, and M. Serbyn, Colloquium: Many-body localization, thermalization, and entanglement, *Rev. Mod. Phys.* **91**, 021001 (2019).

- [35] J. Šuntajs, J. Bonča, T. Prosen, and L. Vidmar, Quantum chaos challenges many-body localization, *Phys. Rev. E* **102**, 062144 (2020).
- [36] J. Šuntajs, J. Bonča, T. Prosen, and L. Vidmar, Ergodicity breaking transition in finite disordered spin chains, *Phys. Rev. B* **102**, 064207 (2020).
- [37] M. Kiefer-Emmanouilidis, R. Unanyan, M. Fleischhauer, and J. Sirker, Evidence for unbounded growth of the number entropy in many-body localized phases, *Phys. Rev. Lett.* **124**, 243601 (2020).
- [38] D. Sels and A. Polkovnikov, Dynamical obstruction to localization in a disordered spin chain, *Phys. Rev. E* **104**, 054105 (2021).
- [39] M. Kiefer-Emmanouilidis, R. Unanyan, M. Fleischhauer, and J. Sirker, Slow delocalization of particles in many-body localized phases, *Phys. Rev. B* **103**, 024203 (2021).
- [40] T. LeBlond, D. Sels, A. Polkovnikov, and M. Rigol, Universality in the onset of quantum chaos in many-body systems, *Phys. Rev. B* **104**, L201117 (2021).
- [41] L. Vidmar, B. Krajewski, J. Bonča, and M. Mierzejewski, Phenomenology of Spectral Functions in Disordered Spin Chains at Infinite Temperature, *Phys. Rev. Lett.* **127**, 230603 (2021).
- [42] D. Sels and A. Polkovnikov, Thermalization of dilute impurities in one dimensional spin chains, [arXiv:2105.09348](https://arxiv.org/abs/2105.09348) (2021).
- [43] B. Krajewski, L. Vidmar, J. Bonča, and M. Mierzejewski, Restoring Ergodicity in a Strongly Disordered Interacting Chain, *Phys. Rev. Lett.* **129**, 260601 (2022).
- [44] R. K. Panda, A. Scardicchio, M. Schulz, S. R. Taylor, and M. Žnidarič, Can we study the many-body localisation transition?, *EPL (Europhysics Letters)* **128**, 67003 (2020).
- [45] P. Sierant, D. Delande, and J. Zakrzewski, Thouless time analysis of anderson and many-body localization transitions, *Phys. Rev. Lett.* **124**, 186601 (2020).
- [46] P. Sierant, M. Lewenstein, and J. Zakrzewski, Polynomially filtered exact diagonalization approach to many-body localization, *Phys. Rev. Lett.* **125**, 156601 (2020).
- [47] D. Ananin, J. Bardarson, G. De Tomasi, S. Gopalakrishnan, V. Khemani, S. Parameswaran, F. Pollmann, A. Potter, M. Serbyn, and R. Vasseur, Distinguishing localization from chaos: Challenges in finite-size systems, *Ann. Phys.* **427**, 168415 (2021).
- [48] Á. L. Corps, R. A. Molina, and A. Relaño, Signatures of a critical point in the many-body localization transition, *SciPost Phys.* **10**, 107 (2021).
- [49] A. Prakash, J. H. Pixley, and M. Kulkarni, Universal spectral form factor for many-body localization, *Phys. Rev. Research* **3**, L012019 (2021).
- [50] J. Schliemann, J. V. I. Costa, P. Wenk, and J. C. Egues, Many-body localization: Transitions in spin models, *Phys. Rev. B* **103**, 174203 (2021).
- [51] M. Hopjan, G. Orso, and F. Heidrich-Meisner, Detecting delocalization-localization transitions from full density distributions, *Phys. Rev. B* **104**, 235112 (2021).
- [52] A. Solórzano, L. F. Santos, and E. J. Torres-Herrera, Multifractality and self-averaging at the many-body localization transition, *Phys. Rev. Research* **3**, L032030 (2021).
- [53] G. De Tomasi, I. M. Khaymovich, F. Pollmann, and S. Warzel, Rare thermal bubbles at the many-body localization transition from the Fock space point of view, *Phys. Rev. B* **104**, 024202 (2021).
- [54] P. J. D. Crowley and A. Chandran, A constructive theory of the numerically accessible many-body localized to thermal crossover, *SciPost Phys.* **12**, 201 (2022).
- [55] R. Ghosh and M. Žnidarič, Resonance-induced growth of number entropy in strongly disordered systems, *Phys. Rev. B* **105**, 144203 (2022).
- [56] N. Bölter and S. Kehrein, Scrambling and many-body localization in the XXZ chain, *Phys. Rev. B* **105**, 104202 (2022).
- [57] Y. Zhang and Y. Liang, Optimizing randomized potentials for inhibiting thermalization in one-dimensional systems, *Phys. Rev. Research* **4**, 023091 (2022).
- [58] P. Sierant and J. Zakrzewski, Challenges to observation of many-body localization, *Phys. Rev. B* **105**, 224203 (2022).
- [59] A. Morningstar, L. Colmenarez, V. Khemani, D. J. Luitz, and D. A. Huse, Avalanches and many-body resonances in many-body localized systems, *Phys. Rev. B* **105**, 174205 (2022).
- [60] J. Sutradhar, S. Ghosh, S. Roy, D. E. Logan, S. Mukerjee, and S. Banerjee, Scaling of the Fock-space propagator and multifractality across the many-body localization transition, *Phys. Rev. B* **106**, 054203 (2022).
- [61] F. B. Trigueros and C.-J. Lin, Krylov complexity of many-body localization: Operator localization in Krylov basis, *SciPost Phys.* **13**, 037 (2022).
- [62] D. Z. Shi, V. Khemani, R. Vasseur, and S. Gopalakrishnan, Many body localization transition with correlated disorder, [arXiv:2204.06017](https://arxiv.org/abs/2204.06017).
- [63] W. De Roeck and F. Huveneers, Stability and instability towards delocalization in many-body localization systems, *Phys. Rev. B* **95**, 155129 (2017).
- [64] D. J. Luitz, F. Huveneers, and W. De Roeck, How a small quantum bath can thermalize long localized chains, *Phys. Rev. Lett.* **119**, 150602 (2017).
- [65] T. Thiery, F. Huveneers, M. Müller, and W. De Roeck, Many-body delocalization as a quantum avalanche, *Phys. Rev. Lett.* **121**, 140601 (2018).
- [66] P. J. D. Crowley and A. Chandran, Avalanche induced coexisting localized and thermal regions in disordered chains, *Phys. Rev. Research* **2**, 033262 (2020).
- [67] D. Sels, Bath-induced delocalization in interacting disordered spin chains, *Phys. Rev. B* **106** (2022).
- [68] J. Šuntajs and L. Vidmar, Ergodicity Breaking Transition in Zero Dimensions, *Phys. Rev. Lett.* **129**, 060602 (2022).
- [69] P. J. D. Crowley and A. Chandran, Mean-field theory of failed thermalizing avalanches, *Phys. Rev. B* **106**, 184208 (2022).
- [70] S. Aubry and G. André, Analyticity breaking and anderson localization in incommensurate lattices, *Ann. Isr. Phys. Soc.* **3**, 133 (1980).
- [71] I. Suslov, Anderson localization in incommensurate systems, *JETP* **56**, 612 (1982).
- [72] M. Kohmoto, Metal-insulator transition and scaling for incommensurate systems, *Phys. Rev. Lett.* **51**, 1198 (1983).
- [73] C. Tang and M. Kohmoto, Global scaling properties of the spectrum for a quasiperiodic schrödinger equation, *Phys. Rev. B* **34**, 2041 (1986).
- [74] M. Kohmoto, B. Sutherland, and C. Tang, Critical wave functions and a cantor-set spectrum of a one-dimensional quasicrystal model, *Phys. Rev. B* **35**, 1020 (1987).

- [75] A. P. Siebesma and L. Pietronero, Multifractal properties of wave functions for one-dimensional systems with an incommensurate potential, *EPL (Europhysics Letters)* **4**, 597 (1987).
- [76] H. Hiramoto and M. Kohmoto, Scaling analysis of quasiperiodic systems: Generalized harper model, *Phys. Rev. B* **40**, 8225 (1989).
- [77] H. Hiramoto and M. Kohmoto, Electronic spectral and wavefunction properties of one-dimensional quasiperiodic systems: A scaling approach, *Int. J. Mod. Phys. B* **06**, 281 (1992).
- [78] E. Maciá, On the nature of electronic wave functions in one-dimensional self-similar and quasiperiodic systems, *ISRN Condensed Matter Physics* **2014**, 165943 (2014).
- [79] X. Li, J. H. Pixley, D.-L. Deng, S. Ganeshan, and S. Das Sarma, Quantum nonergodicity and fermion localization in a system with a single-particle mobility edge, *Phys. Rev. B* **93**, 184204 (2016).
- [80] A.-K. Wu, Fractal Spectrum of the Aubry-Andre Model, [arXiv:2109.07062](https://arxiv.org/abs/2109.07062) (2021).
- [81] G. Roati, C. D'Errico, L. Fallani, M. Fattori, C. Fort, M. Zaccanti, G. Modugno, M. Modugno, and M. Inguscio, Anderson localization of a non-interacting bose-einstein condensate, *Nature* **453**, 895 (2008).
- [82] H. P. Lüschen, S. Scherg, T. Kohlert, M. Schreiber, P. Bordia, X. Li, S. Das Sarma, and I. Bloch, Single-particle mobility edge in a one-dimensional quasiperiodic optical lattice, *Phys. Rev. Lett.* **120**, 160404 (2018).
- [83] Y. Lahini, R. Pugatch, F. Pozzi, M. Sorel, R. Morandotti, N. Davidson, and Y. Silberberg, Observation of a localization transition in quasiperiodic photonic lattices, *Phys. Rev. Lett.* **103**, 013901 (2009).
- [84] B. Kramer and A. MacKinnon, Localization: theory and experiment, *Rep. Prog. Phys.* **56**, 1469 (1993).
- [85] A. MacKinnon and B. Kramer, One-parameter scaling of localization length and conductance in disordered systems, *Phys. Rev. Lett.* **47**, 1546 (1981).
- [86] A. MacKinnon and B. Kramer, The scaling theory of electrons in disordered solids: Additional numerical results, *Z. Phys. B* **53**, 1 (1983).
- [87] K. Slevin and T. Ohtsuki, Critical exponent of the anderson transition using massively parallel supercomputing, *J. Phys. Soc. Jpn.* **87**, 094703 (2018).
- [88] T. Ohtsuki and T. Kawarabayashi, Anomalous diffusion at the anderson transitions, *J. Phys. Soc. Jpn.* **66**, 314 (1997).
- [89] Y. Zhao, D. Feng, Y. Hu, S. Guo, and J. Sirker, Entanglement dynamics in the three-dimensional anderson model, *Phys. Rev. B* **102**, 195132 (2020).
- [90] P. Prelovšek and J. Herbrych, Diffusion in the anderson model in higher dimensions, *Phys. Rev. B* **103**, L241107 (2021).
- [91] F. Evers and A. D. Mirlin, Anderson transitions, *Rev. Mod. Phys.* **80**, 1355 (2008).
- [92] A. Rodriguez, L. J. Vasquez, and R. A. Römer, Multifractal analysis with the probability density function at the three-dimensional anderson transition, *Phys. Rev. Lett.* **102**, 106406 (2009).
- [93] A. Rodriguez, L. J. Vasquez, K. Slevin, and R. A. Römer, Critical parameters from a generalized multifractal analysis at the anderson transition, *Phys. Rev. Lett.* **105**, 046403 (2010).
- [94] G. Schubert, A. Weiße, G. Wellein, and H. Fehske, Hqs@hpc: Comparative numerical study of anderson localization in disordered electron systems, *High Performance Computing in Science and Engineering, Garching 2004*, edited by A. Bode and F. Durst, 237-249 (Springer Berlin Heidelberg, Berlin, Heidelberg, 2005).
- [95] Random matrix  $R$  is drawn from the GOE ensemble:  $R = \beta(A + A^T)/2 \in \mathbb{R}^{2^N \times 2^N}$  where  $A_{ij} = \text{norm}(0, 1)$  with  $\text{norm}(0, 1)$  random numbers drawn from a normal distribution with zero mean and unit variance. We set  $\beta = 0.3$  as in Refs. [64, 68]. The resulting matrix is embedded to matrix of the full dimension  $2^{N+L}$  by Kronecker product  $\hat{R} = R \otimes \mathcal{I}$  where  $\mathcal{I}$  is the identity matrix of dimension  $2^L$ .
- [96] See Supplemental Material for the finite-size analysis of survival probability in the avalanche model, connection of survival probability with the spectral form factor, and survival probability in the 1D Aubry-Andre model for quantum quenches from initial states that are plane waves.
- [97] J. Šuntajs, T. Prosen, and L. Vidmar, Spectral properties of three-dimensional Anderson model, *Ann. Phys.* **435**, 168469 (2021).
- [98] A. del Campo, J. Molina-Vilaplana, and J. Sonner, Scrambling the spectral form factor: Unitarity constraints and exact results, *Phys. Rev. D* **95**, 126008 (2017).

## Supplemental Material: Scale invariant survival probability at eigenstate transitions

Miroslav Hopjan<sup>1</sup> and Lev Vidmar<sup>1,2</sup>

<sup>1</sup>*Department of Theoretical Physics, J. Stefan Institute, SI-1000 Ljubljana, Slovenia*

<sup>2</sup>*Department of Physics, Faculty of Mathematics and Physics, University of Ljubljana, SI-1000 Ljubljana, Slovenia*

### S1. SURVIVAL PROBABILITY IN THE AVALANCHE MODEL

In Fig. S1 we show the survival probability  $p(\tau)$  at the transition point  $\alpha = 0.75$  of the avalanche model. For clarity we only consider the three largest system sizes  $L = 11, 12, 13$ . By increasing  $L$ , one can observe the development of a scale invariant regime of  $p(\tau)$ . The time window in which  $p(\tau)$  is described by a power-law (dashed line) for the largest system size is highlighted by the shaded area.

For system sizes  $L = 11, 12$  we average over 500 Hamiltonian realizations. For the largest system size  $L = 13$ , where the size of the Hamiltonian matrix is  $D = 2^{L+N} = 65536$ , convergence is obtained by applying 150 Hamiltonian realizations. This means that for  $L = 13$  the averaging is performed over  $150 \times 65536 \approx 10^7$  initial states.

We note that convergence of the spectral form factor (discussed below) requires averaging over larger number of Hamiltonian realizations as there is only one data set per Hamiltonian realization. For  $L = 13$ , satisfactory convergence is obtained by averaging over 5000 Hamiltonian realizations.

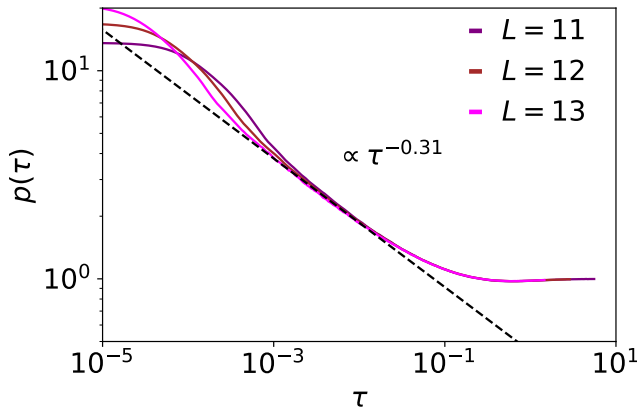


FIG. S1. Survival probability  $p(\tau)$  as a function of the scaled time  $\tau = t/t_H^{\text{typ}}$  in the avalanche model at the transition point  $\alpha = 0.75$ , for three different system sizes  $L = 11, 12, 13$  [the same results as in Fig. 3(b) of the main text].

### S2. CONNECTION TO THE SPECTRAL FORM FACTOR

We next compare the behaviour of the survival probability  $p(\tau)$  shown in the main text to the behaviour of the spectral form factor (SFF). Recently, the characterisation of the eigenstate transitions using the SFF has been carried out for the 3D Anderson model [97] and the avalanche model [68]. We note that, therein, the SFF was defined using unfolded spectra and a Gaussian filtering function. In both studies a broad plateau of the SFF at the transition was found and therefore the SFF universality at the transition has been conjectured [68].

Here we consider the raw SFF computed from the raw Hamiltonian eigenvalues,

$$K_R(t) = \left\langle \left| \sum_{\nu=1}^D e^{-iE_\nu t} \right|^2 \right\rangle_H, \quad (\text{S1})$$

where  $\langle \dots \rangle_H$  denotes the average over Hamiltonian realizations, and no spectral unfolding and filtering function are applied. We show that, still, the SFF defined in this way retains the universality observed in Refs. [68, 97]. The reason to use the raw SFF  $K_R(t)$  is that it naturally connects to the survival probability  $p(t)$  in Eq. (3).

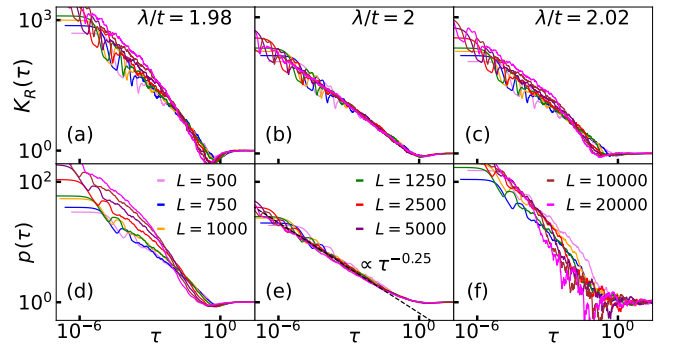


FIG. S2. (a)-(c) The raw SFF  $K_R(\tau)$  from Eq. (S1) as function of the scaled time  $\tau = t/t_H^{\text{typ}}$  in the 1D Aubry-Andree model at different system sizes ( $D = L$ ), plotted (a) in the delocalized regime, (b) at the transition point, and (c) in the localized regime. (d)-(f) The corresponding survival probability  $p(\tau)$  [the same results as in Fig. 1 of the main text]. The shaded areas in (b) and (e) denote the time interval of the power-law behavior of  $K_R(\tau)$  and  $p(\tau)$  for the largest system size  $L = 20000$ .



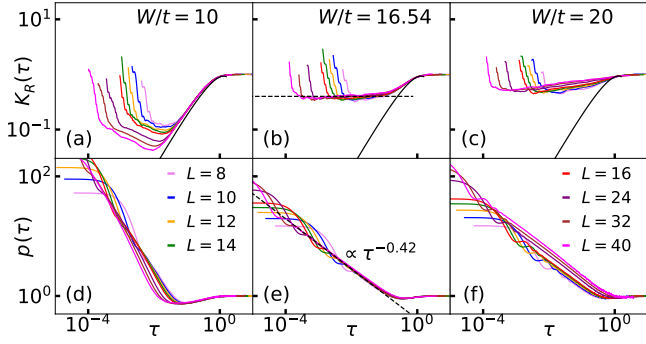


FIG. S3. (a)-(c) The raw SFF  $K_R(\tau)$  from Eq. (S1) as function of the scaled time  $\tau = t/t_H^{\text{typ}}$  in the 3D Anderson model at different system sizes ( $D = L^3$ ), plotted (a) in the delocalized regime, (b) at the transition point, and (c) in the localized regime. The solid line in (b) denotes the GOE result  $K_{\text{GOE}}(\tau) = 2\tau - \tau \ln(1 - 2\tau)$ , while the dashed line in (b) denotes a plateau of  $K_R(\tau)$ . (d)-(f) The corresponding survival probability  $p(\tau)$  [the same results as in Fig. 2 of the main text]. The shaded areas in (b) and (e) denote the time interval of the plateau in  $K_R(\tau)$  and the power-law behavior of  $p(\tau)$ , respectively, for the largest system size  $L = 40$ .

Indeed,  $K_R(t)$  can be interpreted as  $p(t)$  where each initial state  $|m\rangle$  in Eq. (1) is replaced with the infinite-temperature pure state  $|m_{T=\infty}\rangle = \sum_{\nu} D^{-1/2} |\nu\rangle$ . Then, the values of long-time limits in Eq. (3) are  $\bar{P} = 1/D$  and  $P_{\infty} = 0$ , and  $p(t)$  hence reduces to  $K_R(t)$ . To discuss the connection to scale invariance of  $p(\tau)$ , we plot the SFF  $K_R$  as a function of the scaled time  $\tau = t/t_H^{\text{typ}}$ .

In Figs. S2(a)-S2(c) we plot the raw SFF  $K_R(\tau)$  for the 1D Aubry-Andre model and compare it to the survival probability  $p(\tau)$ , see Figs. S2(d)-S2(f), which contain the same results as Fig. 1 of the main text. We observe that at the transition point, see Figs. S2(b) and S2(e), the scale invariant power-law behavior in  $p(\tau)$  is accompanied by a similar behavior in  $K_R(\tau)$ . Away from the transition, see Figs. S2(a) and S2(c), such scale invariance is lost. We note that the power-law behavior in  $K_R(\tau)$  in Fig. S2(b) in the 1D Aubry-Andre model is different from behavior in the 3D Anderson model and the avalanche model, which we discuss below.

In Fig. S3, we compare the raw SFF  $K_R(\tau)$  and  $p(\tau)$  in the 3D Anderson model. The results for  $p(\tau)$  are the same as in Fig. 2 in the main text. The behaviour of the SFF was discussed in Ref. [97]. This is, below the transition, the SFF follows the GOE prediction for times larger than the Thouless time. More importantly, at the transition, the SFF exhibits a broad plateau before it reaches the Thouless time. This is also observed here for the raw SFF, see Figs. S3(a)-S3(c). Below the transition, the raw SFF  $K_R(\tau)$  also approaches the GOE prediction with a small deviation, the latter being an artefact of using the raw spectrum. At the transition a broad plateau is observed, see Fig. S3(b). Remarkably, the time window of the broad scale invariant plateau in  $K_R(\tau)$  almost

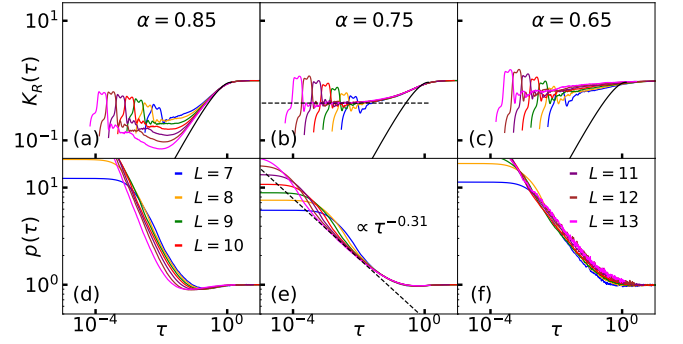


FIG. S4. The raw SFF  $K_R(\tau)$  from Eq. (S1) as function of the scaled time  $\tau = t/t_H^{\text{typ}}$  in the avalanche at different system sizes ( $D = 2^{N+L}$ ), plotted (a) in the delocalized phase, (b) at the transition point, and (c) in the localized phase. The black lines denotes the GOE result  $K_{\text{GOE}}(\tau) = 2\tau - \tau \ln(1 - 2\tau)$ . The dashed line in (b) denotes a plateau of  $K_R(\tau)$ . (d)-(f) The corresponding survival probability  $p(\tau)$  [the same results as in Fig. 3 of the main text]. The shaded area denotes the time interval of the plateau in  $K_R(\tau)$  and the power-law behavior of  $p(\tau)$ , respectively, for the largest system size  $L = 13$ .

exactly corresponds to the time window of the scale invariant power-law decay of  $p(\tau)$  observed in Fig. S3(e).

Finally, in Fig. S4, we compare the raw SFF  $K_R(\tau)$  with  $p(\tau)$  for the avalanche model. The results for  $p(\tau)$  are the same as in Fig. 3 in the main text. Compared to the 3D Anderson model, the features are qualitatively similar. For the avalanche model, the behaviour of the SFF was discussed in Ref. [68]. Also for this model, in the ergodic phase, the SFF follows the GOE prediction for times larger than the Thouless time, and at the transition the scale invariant plateau emerges. The same features are visible in the raw SFF  $K_R(\tau)$ , see Figs. S4(a)-S4(c). At the transition a broad plateau is observed, see Fig. S4(b). As in the case of the 3D Anderson model, in the avalanche model the time window of the broad scale invariant plateau in  $K_R(\tau)$  almost exactly corresponds to the time window of the scale invariant power-law decay of  $p(\tau)$  observed in Fig. S4(e).

### S3. QUENCHES IN THE 1D AUBRY-ANDRE MODEL FROM INITIAL PLANE WAVES

In Fig. S5, we again compare the raw SFF  $K_R(\tau)$  with  $p(\tau)$  in the 1D Aubry-Andre model, as in Fig. S2. However, in this case we consider initial conditions for  $p(\tau)$  that are delocalized plane waves, i.e., we quench from single-particle eigenstates of  $\hat{H}_0 = -t \sum_{\langle ij \rangle} (\hat{c}_i^\dagger \hat{c}_j + \hat{c}_j^\dagger \hat{c}_i)$ . In spite of this change of initial conditions, one may draw similar conclusions about scale invariance of  $K_R(\tau)$  and  $p(\tau)$  at the transition, since the latter takes place in nearly identical time interval as in Fig. S2. Moreover, the exponent  $\beta$  of the power-law decay is very similar in both cases: we get  $\beta = 0.25$  in Fig. S2 and  $\beta = 0.27$  in

Fig. S5.

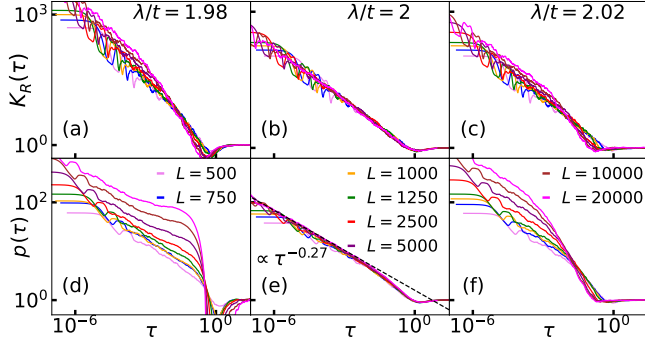


FIG. S5. The raw SFF  $K_R(\tau)$  from Eq. (S1) as function of the scaled time  $\tau = t/t_H^{\text{typ}}$  in the 1D Aubry-Andre model at different system sizes ( $D = L$ ), plotted (a) in the delocalized regime, (b) at the transition point, and (c) in the localized regime. (d)-(f) The corresponding survival probability  $p(\tau)$ , for which the initial states are single-particle plane waves, as described in the text. The dashed line in (e) denotes the power-law fit  $p(\tau) = a\tau^{-\beta}$  to the results at the transition, and we obtain  $\beta = 0.27$ . The shaded areas in (b) and (e) denote the time interval of the power-law behavior of  $K_R(\tau)$  and  $p(\tau)$  for the largest system size  $L = 20000$ .